Urban Climate xxx (xxxx) 101914

Contents lists available at ScienceDirect

Urban Climate

journal homepage: www.elsevier.com/locate/uclim

Identifying the mechanisms by which irrigation can cool urban green spaces in summer

Pui Kwan Cheung [a,*], Naika Meili [b], Kerry A. Nice [c], Stephen J. Livesley [a]

[a] School of Agriculture, Food and Ecosystem Sciences, Burnley Campus, University of Melbourne, 500 Yarra Boulevard, Richmond, VIC 3121, Australia
[b] Department of Civil and Environmental Engineering, National University of Singapore, Singapore, Singapore
[c] Transport, Health, and Urban Systems Research Lab, Faculty of Architecture, Building, and Planning, the University of Melbourne, Parkville, VIC 3010, Australia

ARTICLE INFO

Keywords:
Irrigation
Urban green space
Cooling
Surface energy balance
Evapotranspiration
Irrigation amount

ABSTRACT

High temperatures in summer can prevent people from using urban green spaces. Irrigating urban green spaces is a promising strategy to reduce temperatures. In this study, we aimed to a) identify the proportional contribution of different irrigation cooling mechanisms and b) quantify the impacts of different irrigation amounts (from 2 to 30 mm d^{-1}) on the cooling effect of irrigating turfgrass in Melbourne, Australia. We first used a field experiment in Melbourne to provide empirical data to calibrate and verify the performance of an urban ecohydrological model, UT&C. Then, we used UT&C to predict the impacts of irrigating turfgrass on evapotranspiration, the energy balance and microclimate. UT&C predicted that irrigating turfgrass 4 mm d^{-1} would increase the evaporation from grass canopy and soil surface by 0.2 and 0.6 mm d^{-1}, respectively, whereas it would reduce transpiration by 0.6 mm d^{-1} due to intercepted water covering part of the grass canopy following the irrigation. UT&C predicted that daytime (10:00–16:59) mean air temperature reductions would increase from 0.2 to 0.4 °C when the irrigation amount increased from 2 to 4 mm d^{-1}. However, increasing the irrigation amount beyond 4 mm d^{-1} would not increase the cooling benefits.

1. Introduction

Urban green spaces are important for physical and social activities in cities. The use of urban green spaces is strongly dependent on the thermal conditions of the space (Cheung and Jim, 2018) and high temperatures in summer can prevent people from using urban green spaces (Hao et al., 2023). Various mitigation strategies have been proposed to reduce the air temperature of urban green spaces in summer and these strategies can be divided into four major types (Lai et al., 2019): provision of shade, addition of vegetation, modification of surface reflectivity and water-based cooling. While the first three strategies have been widely studied in the past few decades (Santamouris et al., 2017), water-based cooling has received much less attention.

Irrigating urban green spaces is a promising water-based cooling strategy for cities (Coutts et al., 2013; Livesley et al., 2021). To make such a strategy acceptable it is important to make use of alternative water sources (e.g. stormwater harvesting, recycled waste water) so that cooling is not promoted at the cost of potable water resources. Stormwater harvest has been demonstrated to be effective in water saving, particularly in the dry regions (Zhang et al., 2023). A modelling study predicted that irrigating all vegetated sur-

* Corresponding author at: Main Building, Burnley Campus, University of Melbourne, Richmond 3121, Australia.
E-mail address: puikwanc@student.unimelb.edu.au (P.K. Cheung).

https://doi.org/10.1016/j.uclim.2024.101914
Received 14 June 2023; Received in revised form 6 February 2024; Accepted 4 April 2024
2212-0955/

faces in the metropolitan region of Sydney, Australia could reduce daily mean air temperature by 0.5 °C during a heatwave (Gao et al., 2020). In comparison, under normal summer conditions, irrigating turf has been measured to reduce daytime mean air temperature in small urban green spaces by 0.6 °C in Melbourne, Australia (Cheung et al., 2022a). The cooling effect of irrigation can be best understood and explained by analysing the surface energy balance. On a homogenous turf surface, the energy balance can be expressed as:

$$Q^* + Q_f = Q_E + Q_H + \Delta Q_S \ \left(W\ m^{-2}\right) \quad (1)$$

where Q^* is the all-wave net radiation [W m^{-2}], Q_f the anthropogenic heat flux [W m^{-2}], Q_E the latent heat flux [W m^{-2}], Q_H the sensible heat flux [W m^{-2}] and ΔQ_S the net storage heat flux [W m^{-2}] (Oke, 1988). Most modelling studies predicted that irrigation would reduce air temperature as a result of a reduction in sensible heat flux and an increase in latent heat flux through evapotranspiration (Gao et al., 2020; Wang et al., 2019). Evapotranspiration can be partitioned into evaporation from wet surfaces and transpiration (Kool et al., 2014). For a surface covered by grass, evaporation can occur for water on the grass canopy, ponded surface water or soil water evaporated through the soil surface (Meili et al., 2020). The proportional contribution of these evaporation and transpiration processes to an increase in latent heat flux when irrigating urban green spaces has not been adequately simulated. This is because many urban canopy models over-simplify plant physiological processes and sometimes omit some interactions between vegetation and hydrology (Meili et al., 2020). Partitioning evapotranspiration into its constituent evaporation and transpiration processes is important to understand the mechanism leading to the irrigation cooling effect and predict the magnitude of such.

Irrigation amount is a key factor that influences the level of cooling benefit received by irrigating urban green spaces (Cheung et al., 2022b). As opposed to agricultural irrigation which aims to maximise plant water use efficiency (Zhang et al., 2022b), urban green space irrigation can be used to maximise the cooling benefits in these green spaces in addition to meeting plant water requirements. A modelling study in Adelaide, Australia predicted that the relationship between daily mean air temperature reduction and irrigation amount was almost linear, providing 0.5 °C from 5 mm d^{-1} up to 1.8 °C cooling from 15 mm d^{-1} during a heatwave (Broadbent et al., 2018). The same study predicted that additional cooling benefits from increasing irrigation above 15 mm d^{-1} were negligible as evapotranspiration was no longer limited by the supply of soil moisture, but rather the evaporative demand of the atmosphere, i.e., weather conditions. Most studies have focused on the cooling benefits of irrigation during heatwaves (Broadbent et al., 2018; Daniel et al., 2018; Gao et al., 2020) and the impacts of different daily irrigation amounts on the cooling benefits of irrigation in normal summer conditions are not well understood. Since the maximum cooling benefit that can be achieved with a reasonable irrigation amount can vary with background climate and weather conditions (Cheung et al., 2022b), it is important to understand impacts of daily irrigation amount on the cooling benefits of irrigation to inform the management of urban green spaces for optimal cooling.

This study was performed in Melbourne, Australia during the summer months (December–February) which are often warm and dry. Consequently, the soils in unirrigated green spaces can be expected to dry up in summer and reduce the evapotranspiration of vegetation due to soil moisture limitations (Huang and Fry, 2000). One study found that reduced evapotranspiration can make the surface temperature of unirrigated turfgrass as warm as paved surfaces in summer (Spronken-Smith and Oke, 1998). Serious droughts can occur in Melbourne and the last one has lasted for more than a decade from 1997 to 2009 (Grant et al., 2013). Droughts can lead to widespread decline in vegetation health (May et al., 2013) and their ecosystem benefits including their cooling effects in Melbourne (Sanusi and Livesley, 2020). Hence, irrigating urban green spaces in Melbourne is important to sustain the health and evapotranspirative cooling of its vegetation.

In this study, a replicated field experiment was first set up to measure the impacts of irrigating 36 m^2 plots of turf with different amounts of water on microclimate, soil moisture content and soil temperature for two consecutive summers in Melbourne, Australia. The experimental data were used to test and evaluate the performance of a mechanistic urban ecohydrological model, UT&C (Meili et al., 2020). UT&C was subsequently used to model the impacts of irrigating turf on the surface energy balance and evapotranspiration processes, as well as the impacts of different daily irrigation amounts on irrigation cooling benefits in normal summer conditions. This study has two main objectives:

(1) identify the proportional contribution of different irrigation cooling mechanisms; and.
(2) quantify the impacts of different irrigation amounts (from 2 to 30 mm d^{-1}) on the cooling effect of irrigating turfgrass in Melbourne, Australia during normal summer conditions.

This study is unique because a replicated experiment with controlled treatments was conducted to disentangle certain contributory factors and mechanisms of irrigation cooling effect. Both above- and below-ground observations were taken in the experiment to evaluate the performance of UT&C comprehensively. This study can contribute to the development of climate adaptation strategies for cities because it directly measured and assessed the cooling benefits of a promising cooling strategy.

2. Methods and materials

2.1. Experiment to measure impacts of irrigating turf on microclimate and soil temperature

A field experiment was set up at the Burnley Campus of the University of Melbourne, Australia (−37.8, 145.0) to collect testing and model evaluation data. The site is classified as Local Climate Zone B (scattered trees) (Demuzere et al., 2022) under the local climate zone classification system (Stewart and Oke, 2012). The experiment consisted of six identical plots (6 × 6 m, 36 m^2). Three of

the plots were irrigated at 13:00 local time every day and the remaining three were unirrigated. In each plot, four 90° Hunter Rotator nozzles (MP-1000) were installed at the corners and one 360° nozzle at the centre to deliver the irrigation. Since a climate station was installed at the centre of each plot, the nozzles were carefully adjusted such that the water did not hit the sensors of the climate station (Fig. 1). The irrigation volumes were measured by Nymet flow sensors. A 1.8 m tall 70% shade cloth (SOLARSHADE™) was used to enclose the plots to reduce air mixing between the plots and the environment (Fig. 1). The plot ground surface was covered by turfgrass, which was mowed to approximately 50 mm tall every two weeks. The dominant grass species was Kikuyu (*Pennisetum Clandestinum*). The top soil (5–10 cm) was sandy loam (sand:silt:clay = 0.7:0.2:0.1) and the subsoil (50–55 cm) was sandy clay (sand:silt:clay = 0.5:0.1:0.4). The organic matter content of the soil was approximately 0.06 (6%).

In each plot, air temperature, vapour pressure, and wind speed were continuously measured at a height of 1.1 m above the ground and soil moisture content and soil temperature continuously measured at a soil depth of 0.05 m. In one irrigated and one unirrigated plot, incoming and outgoing longwave and shortwave radiation and turf surface temperature were also measured. A reference climate station was located within 30 m of these six experimental plots to provide reference climate conditions and forcing data for the model. All variables were measured every 10 s and 1 min averages were logged. The mean value of a variable between, e.g., 13:00 and 13:59, was registered at 14:00. The measurement heights and specifications of the climate and soil instruments are listed in Table 1. The model testing data set (2021-01-21 to 2021-03-02, 41 days) consisted of one irrigated (4 mm d^{-1}) and one unirrigated plot. The model evaluation data set (2022-01-28 to 2022-03-06, 38 days) consisted of three irrigated and three unirrigated plots; the irrigated plots received 2 mm d^{-1} from 2022 to 01-28 to 2022-02-08 and 4 mm d^{-1} from 2022-02-09 to 2022-03-06. The model testing data set was used to identify the optimal levels of six important parameters for the study site (explained in Section 2.3) and the model evaluation data set was used to evaluate the model performance (explained in Section 2.4).

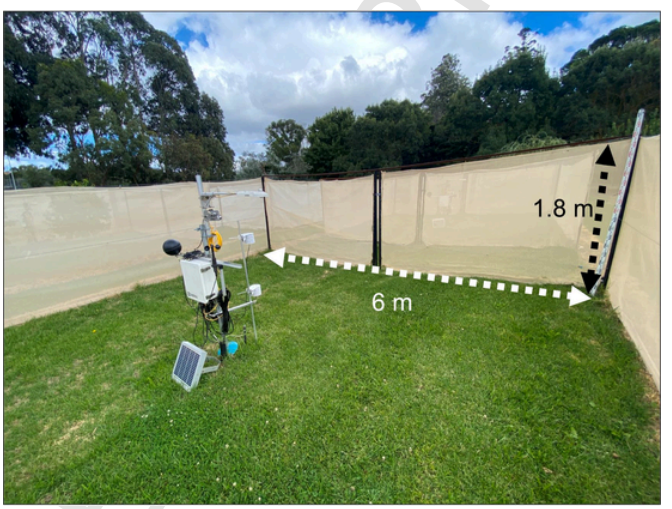

Fig. 1. Six identical plots (6 × 6 m) were set up at the Burnley Campus of the University of Melbourne. Three were unirrigated and three received 4 mm of irrigation at 13:00 every day. Each plot was surrounded by 1.8-m tall 70% shade cloth (SOLARSHADE™) and a climate station was installed at the centre of each plot to continuously monitor the microclimate, soil temperature and soil moisture content.

Table 1
Specifications of the climate and soil instruments.

Location	Model and brand	Variable	Accuracy	Height/depth (m)
Reference	ATMOS14, METER	Air temperature	±0.2 °C	1.1
		Vapour pressure	±1.5% @ 25 °C	1.1
	CNR4, Kipp & Zonen	Incoming longwave radiation (4.5–42 μm)	<10% (daily total)	1.5
		Incoming shortwave radiation (300–2800 nm)	<5% (daily total)	
		Outgoing longwave radiation (4.5–42 μm)	<10% (daily total)	
		Outgoing shortwave radiation (300–2800 nm)	<5% (daily total)	
	CS650, Campbell Scientific	Soil moisture content	±3%	−0.05
		Soil temperature	±1 °C	
	SI-111, Apogee	Turf surface temperature	±0.2 °C (−10 °C to +65 °C)	1.5
	05103, Campbell Scientific	Wind speed	±0.3 m/s	2.0
	HMP155, Campbell Scientific	Air temperature	±(0.055 + 0.0057 × air temperature)	2.0
		Relative humidity	±1%	2.0
	TB4, Campbell Scientific	Rainfall	±2%	2.0

Melbourne has a temperate oceanic climate (Köppen climate classification: Cfb). The mean summer air temperature is 21.0 °C and the mean summer rainfall is 155.3 mm (Bureau of Meteorology, 2023). The mean reference crop evapotranspiration in January in Melbourne is approximately 3.8 mm d^{-1} (City West Water, 2023). In the model testing period, the mean air temperature was 20.0 °C and the total rainfall was 66 mm (Fig. S1). There were eight days with maximum hourly air temperature > 30.0 °C. In the model evaluation period, the mean air temperature was 21.6 °C and the total rainfall was 120.4 mm (Fig. 2). There were 23 days with maximum hourly air temperature > 30.0 °C. The weather in both the model testing period and the model evaluation period was similar to the long-term average weather except the rainfall in the model testing period which was somewhat less than the long-term mean.

2.2. Model description

Urban Tethys-Chloris (UT&C) is a mechanistic model that combines an urban canyon scheme with detailed ecohydrological components (Meili et al., 2020). UT&C solves the energy and water budgets at a neighbourhood scale and the simulation space of UT&C is a two-dimensional infinite urban canyon which is defined by average building height and canyon width. The ground surface can be a combination of vegetated (grass), bare soil and impervious fractions. UT&C can simulate the structural, optical, interception and physiological properties separately for grass and/or trees. Transpiration of grass (and/or trees) is calculated based on meteorological conditions, soil moisture accessed by roots and plant photosynthetic activity (Meili et al., 2020).

UT&C can partition rainfall or sprinkler irrigation into grass canopy interception and throughfall to soil surface. The fraction of water intercepted by plant canopy is calculated following the Rutter model (Fatichi et al., 2012; Rutter et al., 1971). The plant canopy is further divided into a wet and a dry fraction (Deardorff, 1978). Transpiration only occurs from the dry vegetation canopy fraction while evaporation occurs from the wet vegetation canopy fraction. If rainfall or irrigation exceeds the infiltration rate of the soil, ponded surface water is formed which eventually evaporates. Evaporation also occurs from the soil surface below the plant canopy. Effectively, in the absence of trees, UT&C partitions evapotranspiration into four processes, namely evaporation from the wet fraction of the grass canopy, evaporation from soil surface, evaporation from ponding surface water and transpiration from grass. UT&C can simulate sprinkler irrigation (irrigate onto the plant canopy) or drip irrigation (irrigation onto the ground surface) in each time step. UT&C is suitable for our irrigation simulation study because it allows irrigation to be applied onto the plant canopy surface, at a precise time and with a precise amount, includes detailed representations of the interactions between vegetation and hydrology, and enables partitioning of evapotranspiration.

UT&C calculates a) air temperature and vapour pressure at 2 m above ground, b) turf surface temperature and c) soil temperature by solving the urban energy (Eq. (1)) and water (Eq. (2)) budgets:

$$P + Ir = R + E + Lk + \Delta S \ \left(kg\ m^{-2}\ s^{-1}\right) \tag{2}$$

where P is the rainfall [kg m^{-2} s^{-1}], Ir the irrigation [kg m^{-2} s^{-1}], R the surface runoff [kg m^{-2} s^{-1}], E the evapotranspiration [kg m^{-2} s^{-1}], Lk the deep drainage [kg m^{-2} s^{-1}] and ΔS the change in soil water storage [kg m^{-2} s^{-1}]. A detailed model description can be found in Meili et al. (2020).

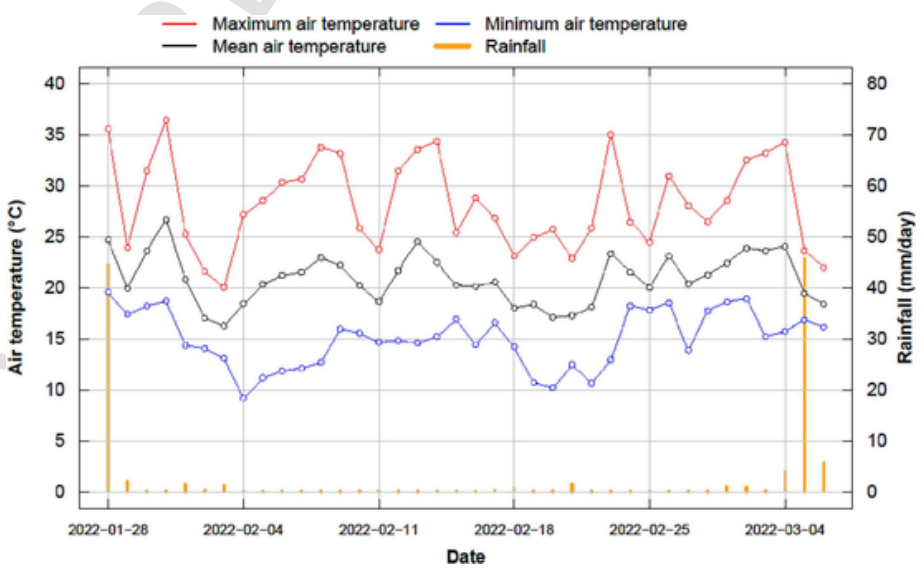

Fig. 2. Daily minimum, mean and maximum air temperatures and rainfall of the model evaluation period (2022-01-28 to 2022-03-06, 38 days).

2.3. Model set up for irrigation study

For our UT&C simulations, we set up a shallow canyon (ground width = 50 m; building height = 5 m) with fully grass-covered ground surface to mimic the open vegetated area of the experimental plots (Table S1). Although the simulation set-up and the experimental plots were different in geometry, the surface energy balance and microclimate were comparable for two reasons. Firstly, the simulated roof heat fluxes in UT&C do not interact with the heat fluxes inside the canyon. Secondly, test simulations indicated that the sensible heat flux from the canyon walls in this wide and shallow canyon set-up had little impact on canyon daytime air temperature (Fig. S4) and daytime and night-time ground surface temperatures inside the canyon (Fig. S5). Furthermore, the capability of UT&C to simulate the surface energy balance and microclimate with a wide and shallow canyon to represent large open green spaces has also been proven in a previous study analysing urban heat islands (Zhang et al., 2022a). Such a UT&C set-up can provide a reasonable approximation of our experimental plots in terms of surface energy balance and microclimate. Since the main analysis in this study considered the microclimatic differences between the irrigated and unirrigated scenarios, the errors arising from the geometric differences would be cancelled out, assuming that the geometric differences affected the two scenarios in a similar way.

The height of the grass was set to 0.1 m which was the average height of the grass during the experiments (Table S2). We used the optical and physiological parameters for grass from Meili et al. (2020), such as canopy light extinction coefficient, root length index, soil water potential at 50% stomatal closure and canopy nitrogen decay coefficient. We also used the soil, interception and runoff parameters from Meili et al. (2020), such as hydraulic conductivity and maximum interception capacity (Table S3). Anthropogenic heat input was assumed to be zero for the site (Table S4). We identified six important parameters that were highly site-specific and tested them to determine the optimal parameter settings to simulate our experiment site. The six parameters are: (i) initial soil moisture content at the start of the simulation, (ii) the depth below which soil moisture content is kept at a fixed value (here at field capacity) [mm], (iii) ground soil composition (i.e. fraction of sand, clay and organic material) [−], (iv) empirical coefficient governing stomatal closure as a function of vapour pressure deficit [Pa], (v) root depth (95th percentile) [mm], and (vi) maximum rubisco capacity at 25 °C at the leaf scale [μmol CO_2 m^{-2} s^{-1}). Four levels of each parameter were used to run the model during the model testing period (2021-01-21 to 2021-03-02, 41 days). Root mean square errors were calculated between the hourly mean modelled air temperature difference between the irrigated and unirrigated scenarios and the measured air temperature differences between the irrigated and unirrigated plots. The level that resulted in the smallest root mean square error (Table S5) or was most representative of the site conditions based on our local knowledge was used in the model evaluation (Section 3.1) and subsequent analysis of the impacts of irrigation on the surface energy balance (Section 3.2) and the impacts of daily irrigation amounts on the cooling benefits (Section 3.3). Instead of calibrating the model separately for the irrigated and unirrigated scenarios, we calibrated the model based on the air temperature difference between the irrigated and unirrigated scenarios because we aimed to quantify the impacts of irrigation on air temperature, which required us to consider both the irrigated and unirrigated scenarios simultaneously.

We used hourly meteorological data to force the model. The forcing data were either directly measured or derived from the measured data and the ERA 5 reanalysis data (Hersbach et al., 2020). Rainfall and incoming shortwave radiation were directly measured at the site (Table 1). The measured data at the reference climate station (2 m above ground) (Fig. 1) and the ERA5 reanalysis data (1000 hPa, ~87 m above ground for the experimental site) were interpolated linearly to obtain the air temperature and relative humidity at 80 m above ground, i.e., the atmospheric reference height of the model. Since we did not have the observational data related to the vertical profile of air temperature, relative humidity and atmospheric pressure, we had to make two assumptions when deriving the forcing data: (i) the vertical profile of air temperature and relative humidity was linear, and (ii) the ERA5 data at 1000 hPa corresponded to exactly a height of 87 m above ground. The altitude relating to atmospheric pressure was calculated according to Portland State Aerospace Society (2004). In reality, the exact height in meters above the surface that corresponds to 1000 hPa is also vary temporally by a small amount. It is also well known that air temperature and relative humidity do not vary linearly with height in the surface layer. ERA5 is not a perfect source of forcing data for this study because of its coarse spatial resolution and poor performance in complex terrain. Nevertheless, the measured data at the reference climate station helped improve the accuracy of the forcing data because it provided a ground truth that reflected the local weather conditions. Wind speed from the measurements at the reference climate station at 2 m was extrapolated to 80 m above ground using the exponential wind profile (Eq. (3)) (Mahat et al., 2013):

$$u(z) = u_h \exp\left[-n\left(1 - \frac{z}{h}\right)\right] \tag{3}$$

u(z) is the wind speed at height *z*, u_h is the wind speed at canopy height *h*, *n* is an exponential decay coefficient. Two sets of forcing data were used, one for the model testing period (2021-01-21 to 2021-03-02, 41 days) (Fig. S6) and one for the model evaluation period (2022-01-28 to 2022-03-06, 38 days) (Fig. S7). Sprinkler irrigation was applied daily at 13:00 local time and the irrigation amount was the same as the experiment, i.e., 4 mm d^{-1} for the model testing period, and 2 mm d^{-1} (2022-01-28 to 2022-02-08) and 4 mm d^{-1} (2022-02-09 to 2022-03-06) for the model evaluation period.

2.4. Model evaluation

The UT&C model was evaluated qualitatively by comparing average diurnal cycles, times series and scatter plots of the modelled output variables to those measured. The UT&C model was also evaluated quantitatively using metrics of coefficient of determination (R^2), mean bias error (MBE), and root mean square error (RMSE). The evaluated model output variables included air temperature

(2 m), vapour pressure (2 m), turf surface temperature and soil temperature (depth = 0–0.1 m). The evaluation was done separately for the irrigated scenario, unirrigated scenario and the difference between the two (irrigated–unirrigated). Since the impacts of irrigation on microclimate and soil temperature were distinctly different in the day and at night, the evaluation was also done separately for daytime (10:00–16:59) and night-time (21:00–05:59) periods where applicable. The model evaluation period was from 2022 to 01-28 to 2022-03-06 (38 days).

There were anomalies in the modelled night-time data in the model evaluation period. The anomalies were due to the failure of the energy balance to converge when the model tried to solve a non-linear equation with multiple variables (Figs. S8 and S9). We excluded the affected periods in the subsequent analysis (31 out of 912 h in Section 3.2 and 56 out of 912 h in Section 3.3).

2.5. Modelling the impacts of irrigating turf on surface energy balance and evapotranspiration processes

The model outputs of latent heat flux, sensible heat flux and soil heat flux of the irrigated and unirrigated scenarios were examined in an average diurnal cycle to understand the impacts of irrigating turf on the surface energy balance. The model outputs also partition evapotranspiration into four processes. The average diurnal cycle of these processes was examined, and their daily means were calculated and compared in a table.

2.6. Modelling the impacts of different daily irrigation amounts on cooling benefits

In a separate simulation, the model was used to predict the impacts of different daily irrigation amounts, namely 2, 4, 6, 8, 15 and 30 mm, on the cooling benefits provided under non-heatwave summer conditions, using an unirrigated scenario as a reference. Sprinkler irrigation was applied daily at 13:00 local time for all six irrigation amounts. The predictions were made using the forcing data of the model evaluation period (2022-01-28 to 2022-03-06, 38 days). The cooling benefits were calculated as the differences in air, turf surface and soil temperatures and air vapour pressure between the irrigated and unirrigated scenarios (Δ = irrigated–unirrigated). The mean daily, daytime (10:00–16:59) and night-time (21:00–05:59) cooling benefits over the whole study period and their 95% confidence intervals were calculated and compared in plots showing the means and error bars. The significance of the cooling benefits was calculated using one sample *t*-tests. An example of the calculation of the cooling benefit of daily mean air temperature is as follows:

$$Cooling\ benefit = \overline{T_{a,irrigated}} - \overline{T_{a,unirrigated}} \quad (4)$$

where $\overline{T_{a,irrigated}}$ is the daily mean air temperature of the irrigated scenario of the study period and $\overline{T_{a,unirrigated}}$ the daily mean air temperature of the unirrigated scenario of the study period.

The workflow of this study is summarised in Fig. 3.

3. Results

3.1. Model evaluation

UT&C predicted the soil moisture content of the irrigated and unirrigated plots well, except after large rainfall events, namely 2022-01-28 (44.4 mm) and 2022-03-05 (45.6 mm) (Fig. 4). Small rainfall events, e.g., 2022-02-18 (0.6 mm), were registered in the modelled soil moisture content at a depth of 0.05 m, but not measured by the soil moisture sensors at the same depth. The soil moisture content of the irrigated and unirrigated plots (scenarios) decreased during the 2-mm irrigation period. The soil moisture content of the irrigated plot (scenario) increased during the 4-mm irrigation period up to a maximum soil moisture content of 35%.

The measured air temperatures, vapour pressures and soil temperatures of the three irrigated plots (Fig. S2) and the three unirrigated plots (Fig. S3) were similar. Therefore, the mean and standard error of the three replicates were used to compare against the modelled results (Fig. S10–S11).

UT&C predicted the average diurnal cycle of air temperature of the irrigated plot well (Fig. S10a). However, the magnitude of air temperature reduction measured at 14:00 due to irrigation was not entirely captured by the model (Fig. S10a). Both the modelled daytime (10:00–16:59) (Fig. S10b) and night-time (21:00–05:59) (Fig. S10c) mean air temperatures closely followed the measured ones. The modelled and measured air temperature were highly correlated in the daytime period (R^2 = 0.93) and moderately correlated in the night-time period (R^2 = 0.69) (Fig. S10 and Table 2). The daytime (night-time) mean bias error and root mean square error of air temperature were – 1.7 °C (–1.2 °C) and 2.1 °C (2.1 °C), respectively. UT&C over-predicted the vapour pressure of the irrigated plot throughout the day (Fig. S10e–h). The modelled and measured vapour pressure were moderately correlated in the daytime (R^2 = 0.73) and night-time (R^2 = 0.45) periods (Table 2). The daytime (night-time) mean bias error and root mean square error of vapour pressure were 0.4 kPa (0.2 kPa) and 0.5 kPa (0.3 kPa), respectively. UT&C predicted the turf surface temperature of the irrigated plot well (Fig. S10g–l). However, the sharp reduction at 14:00 due to irrigation was only captured by the measurement but not the model (Fig. S10g). The modelled and measured turf surface temperature were more highly correlated in the daytime period (R^2 = 0.89) than night-time period (R^2 = 0.60) (Table 2). The daytime (night-time) mean bias error and root mean square error of turf surface temperature were – 1.0 °C (0.9 °C) and 1.7 °C (2.2 °C), respectively. UT&C under-predicted the soil temperature of the irrigated plot, particularly during the night-time (Fig. S10m–p). The modelled and measured soil temperature were moderately corre-

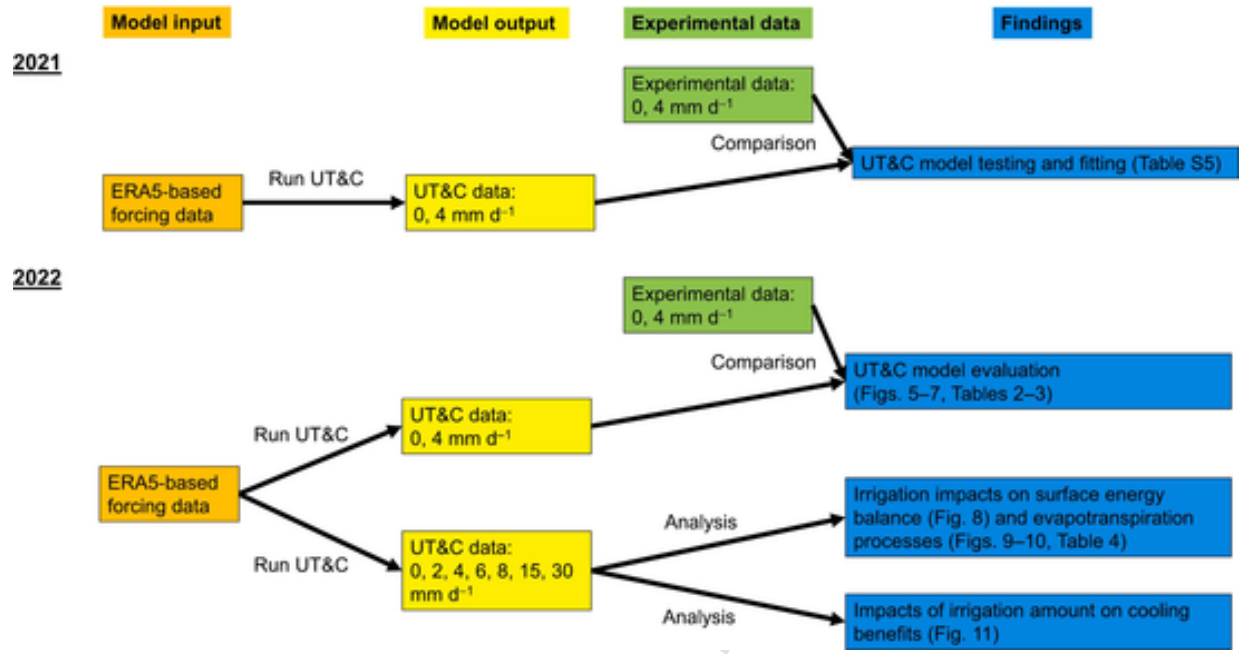

Fig. 3. Workflow of this study. The 2021 experimental data were used to test the UT&C model and identify the best-fit parameters, which were used in the subsequent simulations of 2022. The 2022 experimental data were used for model evaluation for air temperature, vapour pressure, turf surface temperature and soil temperature. From the model evaluation dataset, the irrigation impacts on the surface energy balance and evapotranspiration processes were examined. In a separate simulation using the 2022's forcing data, we examined the impacts of different irrigation amounts on cooling benefits.

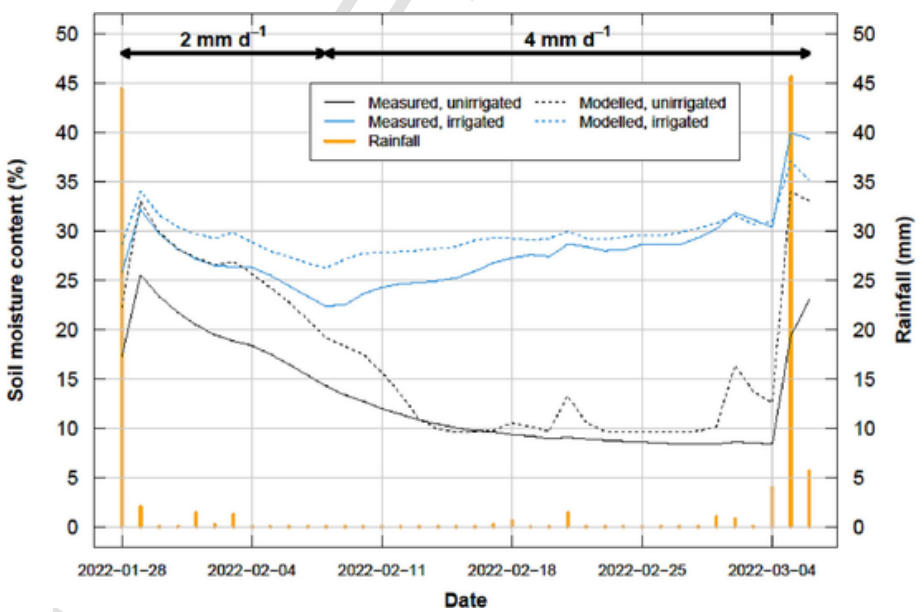

Fig. 4. Comparison of modelled (first soil layer, 0–0.10 m below ground) and measured (0.05 m below ground) daily mean soil moisture content in the model evaluation period (2022-01-28 to 2022-03-06, 38 days). The turf was irrigated 2 mm d^{-1} from 2022 to 01-28 to 2022-02-07 and 4 mm d^{-1} from 2022 to 02-08 to 2022-03-06 at 13:00 local time. In the experiment, the 2-mm irrigation occurred from 13:00 to 13:11, and the 4-mm occurred from 13:00 to 13:23. In the simulation, both 2 and 4 mm were applied to the 13:00–13:59 time step.

lated for both daytime (R^2 = 0.70) and night-time (R^2 = 0.72) periods (Table 2). The daytime (night-time) mean bias error and root mean square error of soil temperature were − 2.0 °C (−5.2 °C) and 2.6 °C (5.4 °C), respectively.

The performance of UT&C in predicting air temperature (Fig. S11a–d), vapour pressure (Fig. S11e–h) and soil temperature (Fig. S11m–p) of the unirrigated plot was similar to that of the irrigated plot (Fig. S10). However, UT&C under-predicted the daytime

Table 2
The performance of UT&C in predicting the daytime (10:00–16:59) and night-time (21:00–05:59) hourly mean air temperature, vapour pressure, turf surface temperature and soil temperature of the irrigated scenario and unirrigated scenario, as well as the differences between the irrigated and unirrigated scenarios. The model performance is evaluated by coefficient of determination (R^2), mean bias error (MBE) and root mean square error (RMSE). The evaluation period was from 2022 to 01-28 to 2022-03-06 (912 h).

			Daytime (10:00–16:59)			Night-time (21:00–05:59)		
	Variable	Unit	R^2	MBE	RMSE	R^2	MBE	RMSE
Irrigated	Air temperature	°C	0.93	−1.7	2.1	0.69	−1.2	2.1
	Vapour pressure	kPa	0.73	0.4	0.5	0.45	0.2	0.3
	Turf surface temperature	°C	0.89	−1.0	1.7	0.60	0.9	2.2
	Soil temperature	°C	0.70	−2.0	2.6	0.72	−5.2	5.4
Unirrigated	Air temperature	°C	0.92	−2.1	2.5	0.68	−1.1	2.1
	Vapour pressure	kPa	0.73	0.4	0.5	0.45	0.2	0.3
	Turf surface temperature	°C	0.88	−3.2	3.7	0.54	1.4	2.7
	Soil temperature	°C	0.66	−1.5	2.4	0.60	−4.9	5.1
Irrigated–Unirrigated	Air temperature	°C	0.29	0.1	0.3	0.01	−0.2	1.1
	Vapour pressure	kPa	0.12	0.1	0.1	0.00	0.0	0.2
	Turf surface temperature	°C	0.19	1.5	2.0	0.03	−0.6	1.5
	Soil temperature	°C	0.08	−0.9	1.0	0.09	−0.6	1.0

(10:00–16:59) and over-predicted the nigh-time (21:00–05:59) turf surface temperatures of the unirrigated scenario to a larger extent (Fig. S11g–l and Table 2).

Regarding the differences between the irrigated and unirrigated turf, i.e., the impacts of irrigation, UT&C predicted the reduction in daytime (10:00–16:59) air temperature well (Fig. 5a–b). The measured and modelled reductions in daytime mean air temperature were − 0.4 °C and − 0.3 °C, respectively (Table 3). UT&C predicted no impact on night-time (21:00–05:59) air temperature by irrigation, while we measured a small increase in night-time air temperature (Fig. 5a and 6c) (Table 3). UT&C predicted an increase in both daytime and night-time vapour pressure by irrigation, while we measured almost no impact on vapour pressure (Fig. 5e–h) (Table 3). UT&C predicted a small reduction in daytime mean turf surface temperature (−0.8 °C), while we measured a large reduction (−2.3 °C) (Fig. 5g) (Table 3). . UT&C predicted the diurnal variation of soil temperature well (Fig. 5m). The mean bias error and root mean square error of daytime air temperature were 0.1 °C and 0.3 °C, respectively (Table 2), which were in the same order of magnitude of the modelled (−0.3 °C) and measured (−0.4 °C) reductions in daytime mean air temperature (Table 3), and the same applied to daytime turf surface temperature.

3.2. Modelling the impacts of irrigating turf on surface energy balance and evapotranspiration processes

UT&C predicted that irrigation increased latent heat flux and reduce sensible heat flux and ground heat flux (less energy flowing into the ground) from approximately 12:00 to 16:59 local time (Fig. 6). At 14:00, irrigation increased latent heat flux by 42.5 W m^{-2} and reduced sensible heat flux and ground heat flux by 13.8 W m^{-2} and 22.0 W m^{-2}, respectively. Irrigation did not change the latent heat flux, sensible heat flux and ground heat flux from 20:00 to 09:59.

UT&C predicted that irrigation increased the daily total evaporation from grass canopy and soil surface by 0.2 and 0.6 mm d^{-1}, respectively (Table 4). Irrigation reduced the daily total transpiration by 0.6 mm d^{-1}. These changes occurred primarily in the two hours after irrigation (13:00–14:59 local time) (Fig. 7). Irrigation had no impact on the daily total evaporation from ponding surface water, which is zero in both scenarios (Table 4). Overall, irrigation increased the total evapotranspiration by 0.2 mm d^{-1} and increased the evaporation to evapotranspiration ratio from 0.06 to 0.30.

The sharp reduction in transpiration in the irrigated scenario occurred from 14:00 to 15:59 local time (Fig. 7c) and coincided with the modelled increase in intercepted water on leaf surfaces (Fig. 8a). Apart from this period, irrigation also slightly reduced transpiration in other times of the day, which is caused by a smaller leaf-to-air vapour pressure deficit (Fig. 8b) due to a lower modelled leaf temperature (= turf surface temperature in UT&C) (Fig. 8c).

3.3. Modelling the impacts of different daily irrigation amounts on cooling benefits

UT&C predicted that irrigation of the simulated amounts (2 to 30 mm d^{-1}) would all significantly reduce daytime (10:00–16:59) mean air temperature ($p < 0.05$) (Fig. 9a). Irrigating 2, 4, 6, 8, 15 and, 30 mm d^{-1} at 13:00 local time would reduce daytime mean air temperature by −0.2 ± 0.0, −0.4 ± 0.1, −0.5 ± 0.1, −0.5 ± 0.1, −0.6 ± 0.1, and − 0.7 ± 0.1 °C, respectively. Irrigation would significantly increase night-time (21:00–05:59) mean air temperature if the irrigation amounts were ≥ 8 mm d^{-1}. Irrigation of these amounts would also significantly increase daily, daytime and night-time mean vapour pressure by a small amount (<0.1 kPa) ($p < 0.05$) (Fig. 9b). UT&C predicted that irrigation of these amounts would significantly reduce daily and daytime mean turf surface temperature ($p < 0.05$) (Fig. 9c). Irrigation of these amounts would also significantly reduce daily, daytime, and night-time mean soil temperature (Fig. 9d), except for night-time mean soil temperature if irrigation amounts were ≥ 15 mm d^{-1}. Overall, an increasing daily irrigation amount would lead to a stronger daytime cooling benefit, but the additional cooling benefits would greatly reduce when the daily irrigation amounts increase beyond 4 mm d^{-1}.

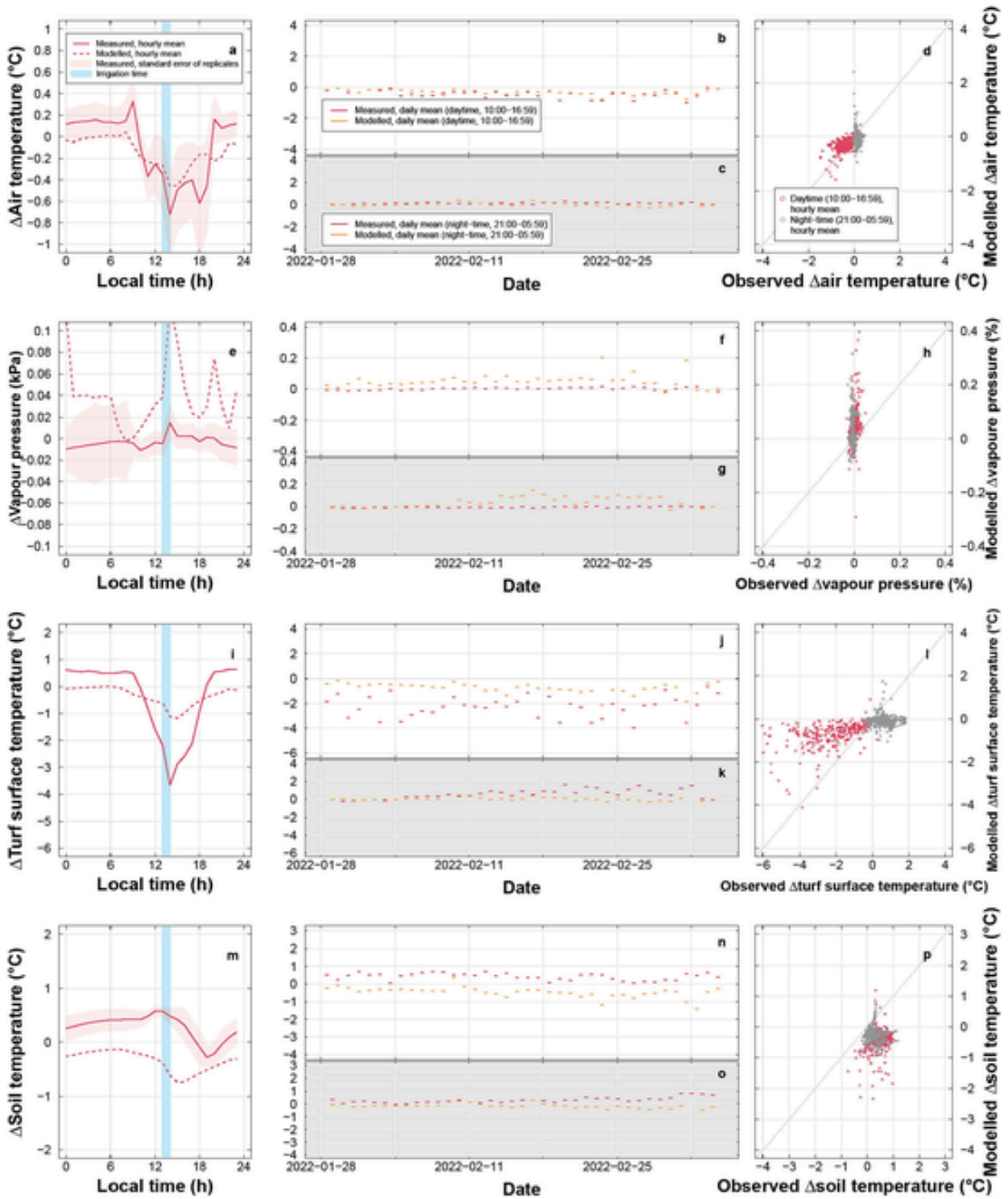

Fig. 5. Model evaluation that compared the modelled differences between the irrigated and unirrigated scenarios (Δ = irrigated – unirrigated) and the measured differences between the irrigated and unirrigated plots in (a–d) air temperature, (e–h) vapour pressure (i–l) turf surface temperature, (m–p) soil temperature. The modelled and measured data were compared in terms of their average diurnal cycles (left column), daytime and night-time daily means (middle column) and scatter plot of hourly means (right column). In the middle column, the broken lines were a time series split into daytime (10:00–16:59, white panels) and night-time (21:00–05:59, grey panels). The model evaluation period was from 2022 to 01-28 to 2022-03-06.

Table 3
The measured and modelled impacts of irrigating turf on daytime (10:00–16:59) and night-time (21:00–05:59) mean air temperature, vapour pressure, turf surface temperature and soil temperature.

		Daytime (10:00–16:59)		Night-time (21:00–05:59)	
Variable	Unit	Measured	Modelled	Measured	Modelled
Air temperature	°C	**−0.4**	**−0.3**	**0.1**	0.0
Vapour pressure	kPa	0.00	**0.05**	**−0.01**	**0.04**
Turf surface temperature	°C	**−2.3**	**−0.7**	**0.6**	0.0
Soil temperature	°C	**−0.4**	**−0.5**	**0.3**	**−0.2**

Significant impacts ($p < 0.05$, *t*-test) are in bold.

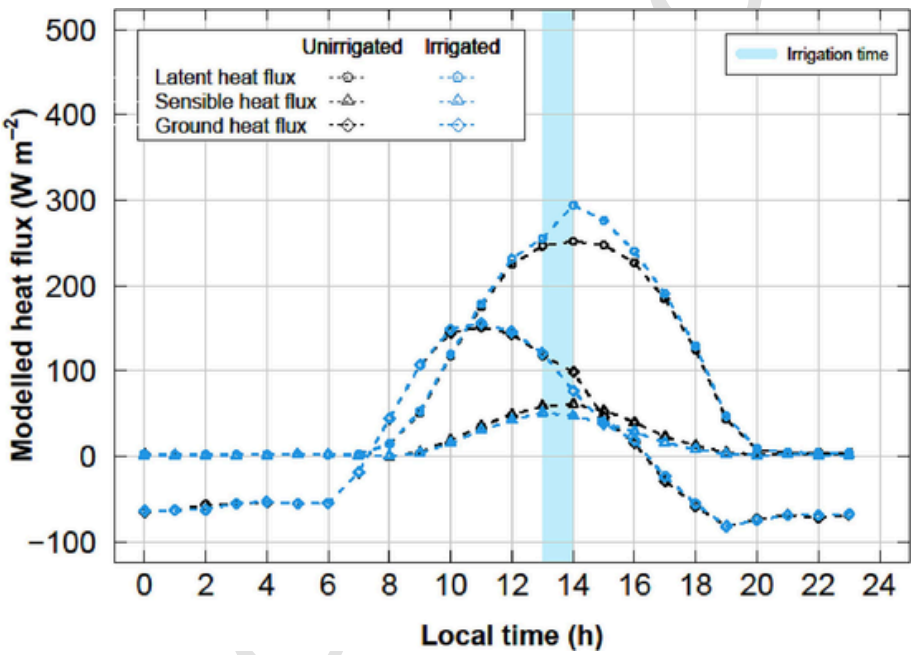

Fig. 6. The average diurnal cycle of modelled latent heat flux, sensible heat flux and ground heat flux of the irrigated and unirrigated scenarios. Irrigation was applied at 13:00, which increased latent heat flux and ground heat flux from 14:00 to 15:59. The data from the model evaluation period (2022-01-28 to 2022-03-06) were used.

Table 4
Modelled mean daily total evaporation from grass canopy, evaporation from soil surface, evaporation from ponding surface water, transpiration and total evapotranspiration of the unirrigated and irrigated scenarios, and the difference between them. The data from the model evaluation period (2022-01-28 to 2022-03-06) were used.

	Daily total (mm)		
Process	Unirrigated scenario	Irrigated scenario	Irrigated–Unirrigated
Evaporation from grass canopy	0.1	0.3	0.2
Evaporation from soil surface	0.1	0.7	0.6
Evaporation from ponding surface water	0.0	0.0	0.0
Transpiration	2.9	2.3	−0.6
Total evapotranspiration	3.1	3.3	0.2

4. Discussion

4.1. Impacts of irrigating turf on surface energy balance and evapotranspiration processes

In this study, both the measurements and the UT&C model agreed that irrigating turf can reduce daytime air and turf surface temperatures. This daytime cooling effect was attributed to an increase in total daytime evapotranspiration. The model predicted that the increase in daytime evapotranspiration was primarily driven by the increase in evaporation from soil surface and from intercepted water on the plant canopy. Other studies have also concluded that irrigating urban vegetated surfaces would increase evapotranspira-

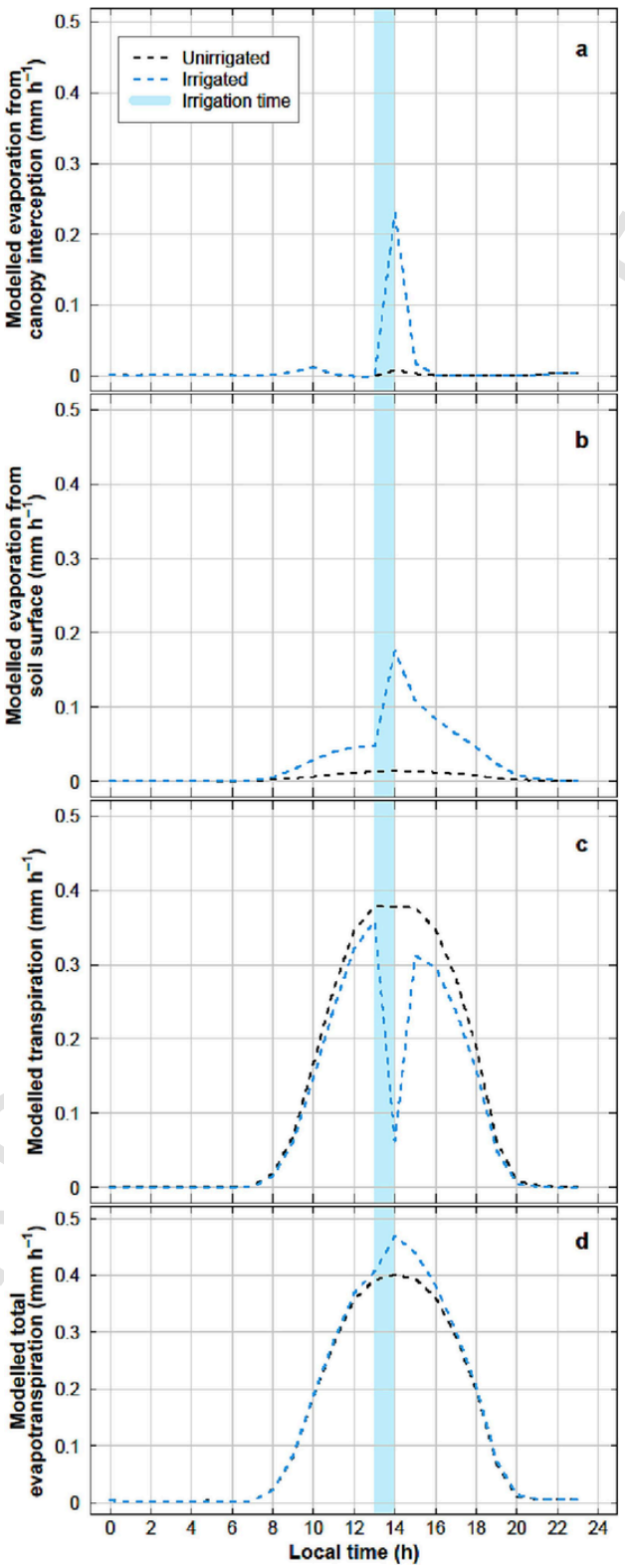
Unirrigated
Irrigated
Irrigation time
a
b
c
d
Modelled evaporation from canopy interception (mm h^{-1})
Modelled evaporation from soil surface (mm h^{-1})
Modelled transpiration (mm h^{-1})
Modelled total evapotranspiration (mm h^{-1})
0
0.1
0.2
0.3
0.4
0.5
0 2 4 6 8 10 12 14 16 18 20 22 24
Local time (h)

Fig. 7. The average diurnal cycle of modelled mean (a) evaporation from grass canopy, (b) evaporation from soil surface, (c) transpiration, and (d) total evapotranspiration. The evaporation from surface water was not plotted because it was always closed to zero. The data from the model evaluation period (2022-01-28 to 2022-03-06) were used.

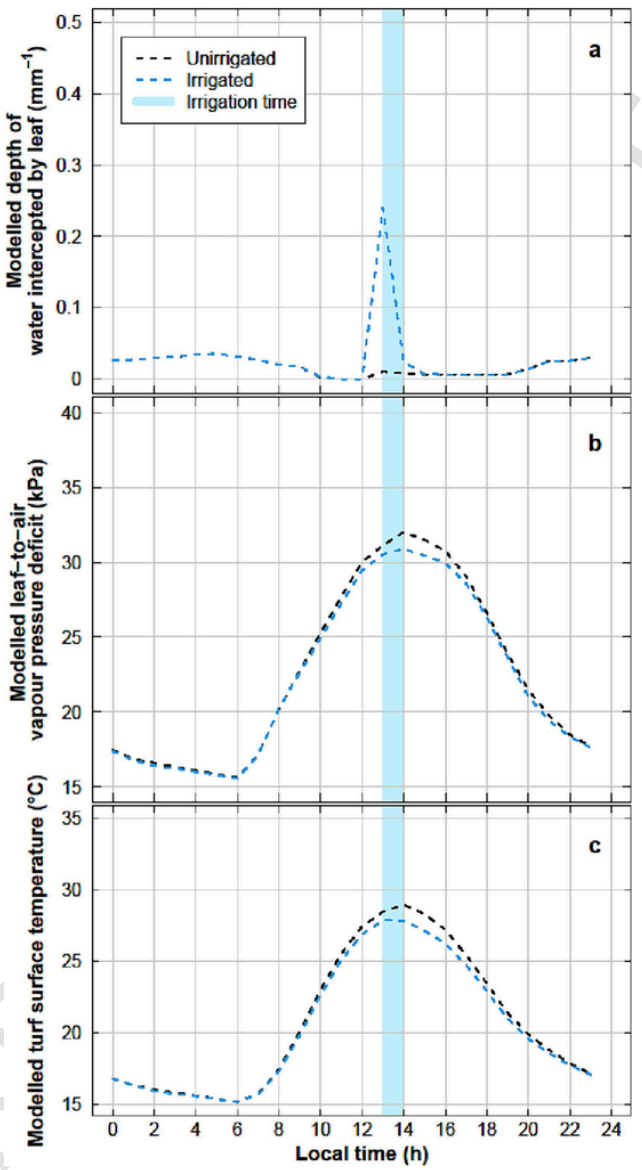

Fig. 8. The average diurnal cycle of modelled (a) depth of water intercepted by leaf, (b) leaf-to-air vapour pressure deficit, and (c) turf surface temperature of the irrigated and unirrigated scenarios. Irrigation was applied at 13:00, which reduced transpiration from 14:00 to 15:59 because transpiration did not occur on the leaf surface with intercepted water in UT&C. Irrigation also reduced transpiration in other times of the day because it reduced leaf-to-air vapour pressure deficit due to reduced leaf temperature (= turf surface temperature in UT&C). The data from the model evaluation period (2022-01-28 to 2022-03-06) were used.

tion (Broadbent et al., 2018; Daniel et al., 2018; Gao et al., 2020). Using the Town Energy Balance model, Daniel et al. (2018) predicted that the increase in daytime evapotranspiration from sprinkler irrigation was primarily driven by an increase in the transpiration of plant (up to 0.2 mm h^{-1}), which was different from the prediction of the UT&C model in the current study. The UT&C model predicted that sprinkler irrigation would reduce the transpiration of turf for two reasons. First, a fraction of the turf canopy would intercept the water and stop transpiring until the intercepted water is evaporated (Meili et al., 2020). In the UT&C model, the plant canopy is divided into a wet and a dry fraction after rainfall or irrigation (Deardorff, 1978). Transpiration only occurs on the dry fraction while evaporation occurs on the wet fraction. The wet fraction may be overestimated in the simulations at the 13:00 timestep when irrigation is applied because part of the sprinkler water is likely to evaporate directly when passing through the air (droplet evaporation) and may not reach the plant canopy as simulated in the model (Fig. 8a). Second, the vegetated ground surface and grass

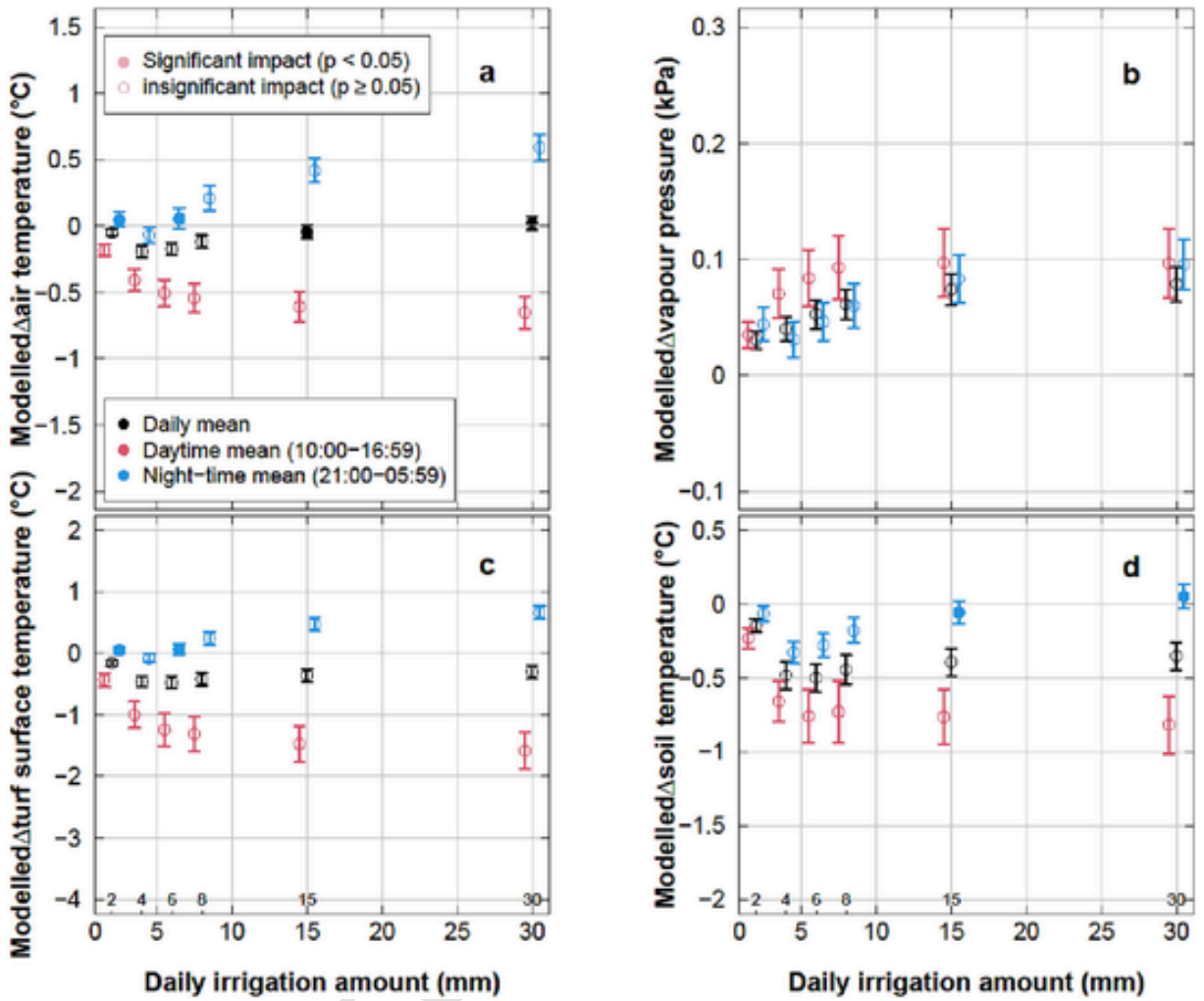

Fig. 9. Modelled impacts of different daily irrigation amount (2, 4, 6, 8, 15 and 30 mm) on (a) air temperature, (b) vapour pressure, (c) turf surface temperature, and (d) soil temperature. The impacts were calculated as the difference between the irrigated and unirrigated scenarios (Δ = irrigated – unirrigated). The circles represented the mean impacts in the simulation period. An open circle represented a significant impact ($p < 0.05$, *t*-test) while a closed circle an insignificant impact ($p \geq 0.05$, t-test). The error bars represent the 95% confident intervals. The overlapping of two error bars is indicative of an insignificant difference ($p \geq 0.05$) between the two means. The forcing data of the model evaluation period (2022-01-28 to 2022-03-06, 38 days) was used in this simulation.

vegetation canopy is modelled with one temperature, which might lead to a larger decrease in modelled vegetation canopy temperature (and leaf-to-air vapour pressure deficit) due to ground evaporation than occurring in reality. Transpiration is reduced with a smaller leaf-to-air vapour pressure deficit (Grossiord et al., 2020). The modelled transpiration rate of the irrigated turf was lower than that of the unirrigated most of the time (Fig. 7c) although the soil moisture content of the irrigated turf was higher throughout the simulation period (Fig. 4), indicating that soil moisture was not limiting transpiration in the simulations of the unirrigated plot.

We measured a strong, instantaneous cooling effect from 13:00 to 13:59 which coincided with the irrigation time (13:00–13:23) (Fig. 6a and g). The measured instantaneous cooling effect was induced by droplet evaporation when the water streams passed through the air and by evaporation of water intercepted by the turf canopy. Droplet evaporation can contribute to 10% of water loss in sprinkler irrigation (Molle et al., 2012). The droplet evaporation in this study was likely to be smaller than traditional sprinkler irrigation because the nozzles used in this study were designed to produce water streams that were less conducive to droplet evaporation. Yet, we measured sharp reductions in air and turf surface temperatures during and immediately after irrigation, suggesting that droplet evaporation could greatly influence microclimate for a short period of time. The reduction in turf surface temperature due to irrigation was underestimated by the model during the day. The turf surface temperature was simultaneously influenced by the radiation budget, the evapotranspiration of plants and the ground heat flux. Without the measurements of all these terms, it was difficult to judge which term(s) caused the underestimation. A more comprehensive measurement campaign is needed to identify the main source of error.

The UT&C model predicted the same instantaneous cooling effect once irrigation had ceased from 14:00 to 14:59. The modelled instantaneous cooling effect was not induced by droplet evaporation because the UT&C model does not include this. The modelled in-

stantaneous cooling effect was driven by the evaporation from grass canopy (Fig. 7a) and the soil surface (Fig. 7b). There have been numerous models developed to predict the direct evaporation during irrigation under different weather conditions for different irrigation methods (Playán et al., 2005). Our experiments suggested that it is necessary to account for droplet evaporation in the climate model to predict the cooling effect of sprinkler irrigation accurately. Moreover, there was a delayed cooling response of one hour because the UT&C model first solved the energy budget then the water budget, hence, the irrigation applied at 13:00 only took effect in the model at 14:00. Finer time steps, e.g., minutes not hours, are required to run the model if the instantaneous cooling effect of irrigation needs to be resolved.

In this study, UT&C predicted that irrigation would reduce ground heat flux (less energy flowing into the ground) from 14:00 to 16:59 due to decreased turf surface temperature (Fig. 6). Furthermore, UT&C predicted that irrigation would have almost no impact on night-time ground heat flux and would not induce night-time warming of air temperature (Fig. 5). However, this is contrary to most modelling studies that have predicted that irrigation would increase ground heat flux (more energy flowing into the ground) during the day because wet soils have a higher thermal conductivity (Kanamaru and Kanamitsu, 2008; Vahmani and Ban-Weiss, 2016; Wang et al., 2019). These studies also predicted that wet soils would store more heat during the day and increase night-time air temperature because more heat is released from the soils at night. Experiment studies confirmed the findings of these modelling studies (Cheung et al., 2022a; Horton and Wierenga, 1983). Ground heat flux is difficult to model because of the lack of detailed observational data and the high diversity of soil composition (Kanamaru and Kanamitsu, 2008). Modelling ground heat flux accurately is important to predict the impacts of irrigation on night-time microclimate because ground heat flux strongly influences the night-time microclimate when latent and sensible heat fluxes are close to zero (Fig. 8). Ground heat flux has a direct impact on soil temperature and the underestimation of soil temperature was stronger during night-time than during the day, suggesting that during the day the ground heat flux reduced the model error. The night-time soil temperature could have been too much influenced by surface cooling. Direct measurement of ground heat flux is needed to determine whether the underestimation of soil temperature was due to inaccurate modelled ground heat flux.

UT&C predicted that irrigation would increase night-time air temperature only when irrigation amount was ≥8 mm d^{-1}. At a lower irrigation amount, e.g., 4 mm d^{-1}, irrigation would reduce ground heat flux (less heat flowing into the soils) during the day due to increased latent heat flux (Fig. 6), causing no night-time warming. As irrigation amount increases to ≥8 mm d^{-1}, both the ground heat flux and the latent heat flux during the day should increase because of increased thermal conductivity and increased evapotranspiration, respectively. The increase in evapotranspiration should be small because atmospheric demand would be the limiting factor of evapotranspiration but not soil moisture content. The increase in ground heat flux is expected to be higher than the increase in latent heat flux during the day, causing a significant release of soil heat and an increase in air temperature at night. More research is required to disentangle the dynamics between soil moisture content, soil heat flux and air temperature.

Overall, the edge effect of the experimental plots may contribute to the discrepancy between the modelled and measured surface energy balance, evapotranspiration, microclimate and soil temperature. Given that the plots were relatively small (6 m × 6 m), the landscape elements such as trees in the site might change the microclimate of the plots through modifying the wind profile and shading and change the soil moisture content through roots. UT&C, in contrast, assumes an idealised canyon with infinite length and homogenous surfaces. The uncertainty in the ERA5 meteorological forcing data also contributes to the large biases in Figs. S10 and S11 between the measured and modelled air temperature. Moreover, UT&C over-predicted vapour pressure in both the irrigated and unirrigated scenarios, which was likely due to the underestimation of turbulent exchange of water vapour from within the urban canyon to the atmosphere above the urban canyon.

4.2. Impacts of different daily irrigation amount on cooling benefits

UT&C predicted that the daily mean air temperature reductions from irrigation would increase when daily irrigation amount increases from 2 to 4 mm but it would not increase greatly beyond 4 mm. This amount is reasonable because the mean reference crop evapotranspiration in Melbourne's summer is approximately 3.8 mm d^{-1} (City West Water, 2023). The reference crop evapotranspiration is the evapotranspiration rate of a grass-covered surface that is not short of water (Allen et al., 1998). The reference crop evapotranspiration is a function of available energy (net radiation – ground heat flux) at the ground surface, wind speed, air temperature and vapour pressure deficit. If extreme weather conditions occur such as heatwaves, the reference crop evapotranspiration in Melbourne will increase to >4 mm d^{-1} and a daily irrigation amount > 4 mm d^{-1} will induce extra cooling benefits. Broadbent et al. (2018) used the SURFEX model to predict that the daily mean air temperature reductions would increase almost linearly from 0.5 to 1.8 °C during a heatwave in Adelaide, Australia as irrigation amount increased from 5 to 15 mm d^{-1}. The maximum and mean air temperatures during the heatwave were 45 °C and 30 °C, respectively. The high air temperature during the heatwave have allowed more evapotranspiration to occur, inducing a stronger cooling effect of irrigation.

For the urban green spaces in heavily built-up urban areas, daily evapotranspiration may be greatly increased by the advected sensible heat from surrounding dry surfaces (Oke, 1979). The daily total evapotranspiration of a well-irrigated park in Sacramento, USA was 130% higher than that of a rural irrigated grass site (Spronken-Smith et al., 2000). The air temperature of the park was approximately 2 °C lower than a nearby paved surface for most of the time during the day. Therefore, the actual daily total evapotranspiration can be higher than the reference crop evapotranspiration in certain urban green spaces. The daily irrigation amount for these urban green spaces needs to be higher than the reference crop evapotranspiration to induce the strongest possible cooling effect. Some of the irrigation water will be directly evaporated whilst passing through the air, as well as evaporated from leaf surfaces when intercepted – none of these processes are considered in the reference evapotranspiration calculations but should be maximised for optimal cooling benefit.

4.3. Implications for using irrigation to cool urban green spaces

This study has demonstrated that irrigating a small urban green space can significantly reduce daytime air temperature, turf surface temperature and soil temperature under non-heatwave summer conditions in a temperate region. The results are only applicable to regions that have similar climate to that of Melbourne because the cooling effect of irrigation is highly dependent on background climate (Cook et al., 2015; Thiery et al., 2017). The cooling effect of irrigation is stronger in regions with a higher air temperature and lower rainfall in summer (Cheung et al., 2021). Irrigating urban green spaces was estimated to reduce mean summer air temperature by 2.3 °C in arid hot desert climate (Köppen climate classification: BWh), whereas irrigating urban green spaces might increase mean summer air temperature by 0.3 °C in Mediterranean dry–warm summer climate (Köppen climate classification: Csb) (Cheung et al., 2021). It is necessary to take background climate into account when assessing the potential of using irrigation to cool urban green spaces.

Water supply is another important consideration when using irrigation to cool urban green spaces. Through water sensitive urban design, non-potable water can be collected and stored in the city to support irrigation. Water sensitive urban designs are the approaches and technologies that aim to retain water in the urban landscapes to meet different purposes such as irrigation (Coutts et al., 2013). For example, housing estates can collect and treat their sewage in a centralised system to provide a collective supply of fit-for-purpose water for irrigation (Gil-Meseguer et al., 2019; South East Water, 2021). De-centralised stormwater storage is also possible for individual households. Individual households can collect stormwater runoff from their roofs through gutters and pipes, and store the water in rainwater tanks for future uses (Mitchell et al., 2007). As stormwater harvesting systems become more affordable and accessible, it is estimated that the new housing projects in Melbourne will increase the city's non-potable water supply by seven times by 2050 (9.8% of the city's water consumption) (Environment and Natural Resources Committee, 2009).

5. Conclusion

The impacts of irrigating an urban green space on microclimate were measured and modelled in this study. The UT&C model can predict the impacts of irrigating a small, turfed urban green space on air temperature well. Irrigation (4 mm d^{-1}) is predicted to increase total evapotranspiration by increasing the evaporation from water intercepted on the plant canopy (0.6 mm d^{-1}) and the evaporation from soil surface (0.2 mm d^{-1}) but also leads to a decrease in transpiration in the hours directly following the sprinkler irrigation due to part of the plant canopy being covered by water. Daytime sensible heat is reduced, causing significant reductions in daytime mean air temperature (−0.4 °C) and turf surface temperature (−2.3 °C). The impacts of irrigation on night-time microclimate, surface energy balance and evapotranspiration are small.

Incorporating all evapotranspiration processes into an urban canopy model is crucial for the model to predict the impacts of irrigating urban green spaces on microclimate and surface energy balance. The droplet evaporation during sprinkler or nozzle irrigation needs to be included in urban canopy models because its contribution to total evapotranspiration is sizeable, particular for daytime irrigation. For a turfed urban green space, the daily irrigation amount that can generate the strongest possible cooling effect on an average summer day without excessive drainage is approximately equivalent to the reference crop evapotranspiration of the background climate in question (4 mm d^{-1} in Melbourne).

CRediT authorship contribution statement

Pui Kwan Cheung: Writing – review & editing, Writing – original draft, Visualization, Validation, Software, Methodology, Investigation, Formal analysis, Data curation, Conceptualization. **Naika Meili:** Writing – review & editing, Software, Methodology, Investigation. **Kerry A. Nice:** Writing – review & editing, Supervision, Methodology. **Stephen J. Livesley:** Writing – review & editing, Supervision, Project administration, Funding acquisition.

Uncited references

Foken, 2006
Kent et al., 2017
Macdonald et al., 1998

Declaration of Generative AI and AI-assisted technologies in the writing process

The authors declare that no generative AI and AI-assisted technologies were used in the writing process.

Declaration of competing interest

The authors declare that they have no known competing financial interests or personal relationships that could have appeared to influence the work reported in this paper.

Data availability

Data will be made available on request.

Acknowledgements

This study is supported by the Commonwealth of Australia through the Cooperative Research Centres program. NM acknowledges the support of the National University of Singapore through the project 'Bridging scales from below: The role of heterogeneities in the global water and carbon budgets', Award No. 22-3637-A0001. K.A.N. is supported by NHMRC/UKRI grant (1194959). P.K.C. is supported by the Australian Government Research Training Program Scholarship, the Cooperative Research Centre for Water Sensitive Cities, Madeleine Selwyn-Smith Memorial Scholarships and the Rowden White Scholarship.

Appendix A. Supplementary data

Supplementary data to this article can be found online at https://doi.org/10.1016/j.uclim.2024.101914.

References

Allen, R.G., Pereira, L.S., Raes, D., Smith, M., 1998. Crop Evapotranspiration - Guidelines for Computing Crop Water Requirements - FAO Irrigation and Drainage Paper 56. Rome, Italy.

Broadbent, A.M., Coutts, A.M., Tapper, N.J., Demuzere, M., 2018. The cooling effect of irrigation on urban microclimate during heatwave conditions. Urban Clim. 23, 309–329. https://doi.org/10.1016/j.uclim.2017.05.002.

Bureau of Meteorology, 2023. Climate statistics for Australian locations: Summary statistics [WWW Document]. URL. http://www.bom.gov.au/jsp/ncc/cdio/cvg/av?p_stn_num=086071&p_prim_element_index=0&p_comp_element_index=0&redraw=null&p_display_type=statistics_summary&normals_years=1991-2020&tablesizebutt=normal. (accessed 6.2.23).

Cheung, P.K., Jim, C.Y., 2018. Subjective outdoor thermal comfort and urban green space usage in humid-subtropical Hong Kong. Energ. Build. 173, 150–162. https://doi.org/10.1016/j.enbuild.2018.05.029.

Cheung, P.K., Livesley, S.J., Nice, K.A., 2021. Estimating the cooling potential of irrigating green spaces in 100 global cities with arid, temperate or continental climates. Sustain. Cities Soc. 71, 102974. https://doi.org/10.1016/j.scs.2021.102974.

Cheung, P.K., Jim, C.Y., Tapper, N., Nice, K.A., Livesley, S.J., 2022a. Daytime irrigation leads to significantly cooler private backyards in summer. Urban Clim. 46, 101310. https://doi.org/10.1016/j.uclim.2022.101310.

Cheung, P.K., Nice, K.A., Livesley, S.J., 2022b. Irrigating urban green space for cooling benefits: the mechanisms and management considerations. Environ. Res. Clim. 1, 015001. https://doi.org/10.1088/2752-5295/ac6e7c.

City West Water, 2023. Best Practice Guidelines for Functional Open Space. Melbourne, Australia.

Cook, B.I., Shukla, S.P., Puma, M.J., Nazarenko, L.S., 2015. Irrigation as an historical climate forcing. Clim. Dyn. 44, 1715–1730. https://doi.org/10.1007/s00382-014-2204-7.

Coutts, A.M., Tapper, N.J., Beringer, J., Loughnan, M., Demuzere, M., 2013. Watering our cities: the capacity for water sensitive urban design to support urban cooling and improve human thermal comfort in the Australian context. Prog. Phys. Geogr. Earth Environ. 37, 2–28. https://doi.org/10.1177/0309133312461032.

Daniel, M., Lemonsu, A., Viguié, V., 2018. Role of watering practices in large-scale urban planning strategies to face the heat-wave risk in future climate. Urban Clim. 23, 287–308. https://doi.org/10.1016/j.uclim.2016.11.001.

Deardorff, J.W., 1978. Efficient prediction of ground surface temperature and moisture, with inclusion of a layer of vegetation. J. Geophys. Res. 83, 1889. https://doi.org/10.1029/JC083iC04p01889.

Demuzere, M., Kittner, J., Martilli, A., Mills, G., Moede, C., Stewart, I.D., van Vliet, J., Bechtel, B., 2022. A global map of local climate zones to support earth system modelling and urban-scale environmental science. Earth Syst. Sci. Data 14, 3835–3873. https://doi.org/10.5194/essd-14-3835-2022.

Environment and Natural Resources Committee, 2009. Inquiry into Melbourne's Future Water Supply. Melbourne, Australia.

Fatichi, S., Ivanov, V.Y., Caporali, E., 2012. A mechanistic ecohydrological model to investigate complex interactions in cold and warm water-controlled environments: 1. Theoretical framework and plot-scale analysis. J. Adv. Model. Earth Syst. 4, 1–31. https://doi.org/10.1029/2011MS000086.

Foken, T., 2006. 50 years of the Monin-Obukhov similarity theory. Boundary-Layer Meteorol. 119, 431–447. https://doi.org/10.1007/s10546-006-9048-6.

Gao, K., Santamouris, M., Feng, J., 2020. On the cooling potential of irrigation to mitigate urban heat island. Sci. Total Environ. 740, 139754. https://doi.org/10.1016/j.scitotenv.2020.139754.

Gil-Meseguer, E., Bernabé-Crespo, M.B., Gómez-Espín, J.M., 2019. Recycled sewage - a water resource for dry regions of southeastern Spain. Water Resour. Manag. 33, 725–737. https://doi.org/10.1007/s11269-018-2136-9.

Grant, S.B., Fletcher, T.D., Feldman, D., Saphores, J.D., Cook, P.L.M., Stewardson, M., Low, K., Burry, K., Hamilton, A.J., 2013. Adapting urban water systems to a changing climate: lessons from the millennium drought in Southeast Australia. Environ. Sci. Technol. 47, 10727–10734. https://doi.org/10.1021/es400618z.

Grossiord, C., Buckley, T.N., Cernusak, L.A., Novick, K.A., Poulter, B., Siegwolf, R.T.W., Sperry, J.S., McDowell, N.G., 2020. Plant responses to rising vapor pressure deficit. New Phytol. 226, 1550–1566. https://doi.org/10.1111/nph.16485.

Hao, T., Chang, H., Liang, S., Jones, P., Chan, P.W., Li, L., Huang, J., 2023. Heat and park attendance: evidence from "small data" and "big data" in Hong Kong. Build. Environ. 234, 110123. https://doi.org/10.1016/j.buildenv.2023.110123.

Hersbach, H., Bell, B., Berrisford, P., Hirahara, S., Horányi, A., Muñoz-Sabater, J., Nicolas, J., Peubey, C., Radu, R., Schepers, D., Simmons, A., Soci, C., Abdalla, S., Abellan, X., Balsamo, G., Bechtold, P., Biavati, G., Bidlot, J., Bonavita, M., Chiara, G., Dahlgren, P., Dee, D., Diamantakis, M., Dragani, R., Flemming, J., Forbes, R., Fuentes, M., Geer, A., Haimberger, L., Healy, S., Hogan, R.J., Hólm, E., Janisková, M., Keeley, S., Laloyaux, P., Lopez, P., Lupu, C., Radnoti, G., Rosnay, P., Rozum, I., Vamborg, F., Villaume, S., Thépaut, J., 2020. The ERA5 global reanalysis. Q. J. R. Meteorol. Soc. 146, 1999–2049. https://doi.org/10.1002/qj.3803.

Horton, R., Wierenga, P.J., 1983. Estimating the soil heat flux from observations of soil temperature near the surface. Soil Sci. Soc. Am. J. 47, 14–20. https://doi.org/10.2136/sssaj1983.03615995004700010003x.

Huang, B., Fry, J.D., 2000. Turfgrass evapotranspiration. J. Crop. Prod. 2, 317–333. https://doi.org/10.1300/J144v02n02_14.

Kanamaru, H., Kanamitsu, M., 2008. Model diagnosis of nighttime minimum temperature warming during summer due to irrigation in the California Central Valley. J. Hydrometeorol. 9, 1061–1072. https://doi.org/10.1175/2008JHM967.1.

Kent, C.W., Grimmond, S., Gatey, D., 2017. Aerodynamic roughness parameters in cities: inclusion of vegetation. J. Wind Eng. Ind. Aerodyn. 169, 168–176. https://doi.org/10.1016/j.jweia.2017.07.016.

Kool, D., Agam, N., Lazarovitch, N., Heitman, J.L., Sauer, T.J., Ben-Gal, A., 2014. A review of approaches for evapotranspiration partitioning. Agric. For. Meteorol. 184, 56–70. https://doi.org/10.1016/j.agrformet.2013.09.003.

Lai, D., Liu, W., Gan, T., Liu, K., Chen, Q., 2019. A review of mitigating strategies to improve the thermal environment and thermal comfort in urban outdoor spaces. Sci. Total Environ. https://doi.org/10.1016/j.scitotenv.2019.01.062.

Livesley, S.J., Marchionni, V., Cheung, P.K., Daly, E., Pataki, D.E., 2021. Water smart cities increase irrigation to provide cool refuge in a climate crisis. Earth's Futur. 9,

1–6. https://doi.org/10.1029/2020EF001806.
Macdonald, R.W., Griffiths, R.F., Hall, D.J., 1998. An improved method for the estimation of surface roughness of obstacle arrays. Atmos. Environ. 32, 1857–1864. https://doi.org/10.1016/S1352-2310(97)00403-2.
Mahat, V., Tarboton, D.G., Molotch, N.P., 2013. Testing above- and below-canopy representations of turbulent fluxes in an energy balance snowmelt model. Water Resour. Res. 49, 1107–1122. https://doi.org/10.1002/wrcr.20073.
May, P.B., Livesley, S.J., Shears, I., 2013. Managing and monitoring tree health and soil water status during extreme drought in Melbourne, Victoria. Arboric. Urban For. 39, 136–145. https://doi.org/10.48044/jauf.2013.019.
Meili, N., Manoli, G., Burlando, P., Bou-Zeid, E., Chow, W.T.L., Coutts, A.M., Daly, E., Nice, K.A., Roth, M., Tapper, N.J., Velasco, E., Vivoni, E.R., Fatichi, S., 2020. An urban ecohydrological model to quantify the effect of vegetation on urban climate and hydrology (UT&C v1.0). Geosci. Model Dev. 13, 335–362. https://doi.org/10.5194/gmd-13-335-2020.
Mitchell, V.G., Deletic, A., Fletcher, T.D., Hatt, B.E., McCarthy, D.T., 2007. Achieving multiple benefits from stormwater harvesting. Water Sci. Technol. 55, 135–144. https://doi.org/10.2166/wst.2007.103.
Molle, B., Tomas, S., Hendawi, M., Granier, J., 2012. Evaporation and wind drift losses during sprinkler irrigation influenced by droplet size distribution. Irrig. Drain. 61, 240–250. https://doi.org/10.1002/ird.648.
Oke, T.R., 1979. Advectively-assisted evapotranspiration from irrigated urban vegetation. Boundary-Layer Meteorol. 17, 167–173. https://doi.org/10.1007/BF00117976.
Oke, T.R., 1988. The urban energy balance. Prog. Phys. Geogr. 12, 471–508. https://doi.org/10.1177/030913338801200401.
Playán, E., Salvador, R., Faci, J.M., Zapata, N., Martínez-Cob, A., Sánchez, I., 2005. Day and night wind drift and evaporation losses in sprinkler solid-sets and moving laterals. Agric. Water Manag. 76, 139–159. https://doi.org/10.1016/j.agwat.2005.01.015.
Portland State Aerospace Society, 2004. A Quick Derivation Relating Altitude to Air Pressure.
Rutter, A.J., Kershaw, K.A., Robins, P.C., Morton, A.J., 1971. A predictive model of rainfall interception in forests, 1. Derivation of the model from observations in a plantation of Corsican pine. Agric. Meteorol. 9, 367–384. https://doi.org/10.1016/0002-1571(71)90034-3.
Santamouris, M., Ding, L., Fiorito, F., Oldfield, P., Osmond, P., Paolini, R., Prasad, D., Synnefa, A., 2017. Passive and active cooling for the outdoor built environment – analysis and assessment of the cooling potential of mitigation technologies using performance data from 220 large scale projects. Sol. Energy 154, 14–33. https://doi.org/10.1016/j.solener.2016.12.006.
Sanusi, R., Livesley, S.J., 2020. London Plane trees (Platanus x acerifolia) before, during and after a heatwave: losing leaves means less cooling benefit. Urban For. Urban Green. 54, 126746. https://doi.org/10.1016/j.ufug.2020.126746.
South East Water, 2021. Aquarevo - A new way of living [WWW Document]. URL. https://southeastwater.com.au/residential/upgrades-and-projects/projects/aquarevo/. (accessed 2.21.22).
Spronken-Smith, R.A., Oke, T.R., 1998. The thermal regime of urban parks in two cities with different summer climates. Int. J. Remote Sens. 19, 2085–2104. https://doi.org/10.1080/014311698214884.
Spronken-Smith, R.A., Oke, T.R., Lowry, W.P., 2000. Advection and the surface energy balance across an irrigated urban park. Int. J. Climatol. 20, 1033–1047. https://doi.org/10.1002/1097-0088(200007)20:9<1033::AID-JOC508>3.0.CO;2-U.
Stewart, I.D., Oke, T.R., 2012. Local climate zones for urban temperature studies. Bull. Am. Meteorol. Soc. 93, 1879–1900. https://doi.org/10.1175/BAMS-D-11-00019.1.
Thiery, W., Davin, E.L., Lawrence, D.M., Hirsch, A.L., Hauser, M., Seneviratne, S.I., 2017. Present-day irrigation mitigates heat extremes. J. Geophys. Res. Atmos. 122, 1403–1422. https://doi.org/10.1002/2016JD025740.
Vahmani, P., Ban-Weiss, G., 2016. Climatic consequences of adopting drought-tolerant vegetation over Los Angeles as a response to California drought. Geophys. Res. Lett. 43, 8240–8249. https://doi.org/10.1002/2016GL069658.
Wang, C., Wang, Z.H., Yang, J., 2019. Urban water capacity: irrigation for heat mitigation. Comput. Environ. Urban. Syst. 78, 101397. https://doi.org/10.1016/j.compenvurbsys.2019.101397.
Zhang, Z., Paschalis, A., Mijic, A., Meili, N., Manoli, G., van Reeuwijk, M., Fatichi, S., 2022a. A mechanistic assessment of urban heat island intensities and drivers across climates. Urban Clim. 44, 101215. https://doi.org/10.1016/j.uclim.2022.101215.
Zhang, G., Shen, D., Ming, B., Xie, R., Hou, P., Xue, J., Wang, K., Li, S., 2022b. Optimizing planting density to increase maize yield and water use efficiency and economic return in the arid region of Northwest China. Agric 12. https://doi.org/10.3390/agriculture12091322.
Zhang, Z., Dobson, B., Moustakis, Y., Meili, N., Mijic, A., Butler, A., Athanasios, P., 2023. Assessing the co-benefits of urban greening coupled with rainwater harvesting management under current and future climates across USA cities. Environ. Res. Lett. 18. https://doi.org/10.1088/1748-9326/acbc90.